

2015•2016  
FACULTEIT INDUSTRIËLE INGENIEURSWETENSCHAPPEN  
*master in de industriële wetenschappen: nucleaire  
technologie*

## Masterproef

The influence of respiratory motion on dose delivery in a mouse lung tumor irradiation using the 4D MOBY phantom

Promotor :  
dr. Brigitte RENIERS  
Prof. dr. ir. FRANK VERHAEGEN

Brent van der Heyden

*Scriptie ingediend tot het behalen van de graad van master in de industriële wetenschappen: nucleaire technologie*

Gezamenlijke opleiding Universiteit Hasselt en KU Leuven

2015•2016

Faculteit Industriële

ingenieurswetenschappen

*master in de industriële wetenschappen: nucleaire  
technologie*

## Masterproef

The influence of respiratory motion on dose delivery in  
a mouse lung tumor irradiation using the 4D MOBY phantom

Promotor :  
dr. Brigitte RENIERS  
Prof. dr. ir. FRANK VERHAEGEN

Brent van der Heyden

*Scriptie ingediend tot het behalen van de graad van master in de industriële  
wetenschappen: nucleaire technologie*

## Preface

During my childhood I grew up in a village with a view of the nuclear power plants in Doel (Beveren, Belgium). After high school I decided to study nuclear engineering at Hasselt University with the intention to work in these nuclear power plants. During my studies in the nuclear sciences I became very interested in the medical part of the education. In my third year I had the chance to participate three weeks in the BELdART2 project to write a bachelor thesis. After the completion of this project I decided to study medical nuclear engineering with the additional course of reactor technology in my master's year.

In my master's year I wanted to do a thesis in a well-established radiotherapy center, Maastrro Clinic (Maastricht, The Netherlands). A new question raised within the 'Small Animal Radiotherapy' research group of Maastrro Clinic. They wanted to know the influence of respiratory motion on dose delivery in a mouse lung tumor irradiation.

I want to thank all the people from Maastrro Clinic for the good atmosphere at the workplace. In particular I am thankful to Stefan van Hoof and Lotte Schyns for their help during my research project.

Finally I wish to thank both my external and internal supervisors Frank Verhaegen and Brigitte Reniers.

Brent van der Heyden



## Table of contents

<b>1</b>	<b>Introduction</b>	<b>1</b>
1.1	Dose perturbation in a moving mouse lung tumor	1
1.2	Contrast-enhanced small animal irradiations	2
<b>2</b>	<b>Methods</b>	<b>3</b>
2.1	4D digital mouse whole body (MOBY) phantom	3
2.2	MOBY simulation cases	5
2.3	SmART-Plan	6
2.3.1	Mean organ doses	8
2.3.2	Time-dependent organ doses	8
2.4	Customized MOBY lung tumor volume	9
2.5	Contrast-enhanced radiotherapy using MOBY	10
<b>3</b>	<b>Results</b>	<b>13</b>
3.1	Respiratory simulations: lung tumor displacement	13
3.2	Respiratory simulations: mean organ doses	13
3.3	Respiratory simulations: time-dependent organ doses	15
3.4	Contrast-enhanced radiotherapy simulations	16
<b>4</b>	<b>Discussion</b>	<b>17</b>
4.1	Dose perturbation in a moving mouse lung tumor	17
4.2	Contrast-enhanced small animal irradiations	18
<b>5</b>	<b>Conclusion</b>	<b>19</b>



## List of tables

Table 1. Treatment and calculation settings of SmART-Plan combined with the MOBY phantom parameters to perform MC dose calculations. ....	7
Table 2: The mass density and atomic constituent weight fractions of the Omnipaque iodine based contrast medium. <sup>4</sup> .....	10
Table 3. Maximum lung tumor displacements of all MOBY simulation cases in the Cartesian coordinate system. ( $TD_{\max}^2=Y^2+Z^2$ ).....	13
Table 4. The expected (static) and obtained (moving) mean dose for the tumor, heart and spinal cord of all simulation cases in both right (R) and left (L) lung. ....	14
Table 5. The calculated mean tumor and heart dose for all seven simulation cases with a planned treatment target dose of 8 Gy. ....	16





## List of figures

- Figure 1. Flow diagram of the procedure to estimate lung tumor dose over time. The computer programs are shown in the rounded yellow rectangles, the methods in the blue rectangles and the parameters or settings in the partially rounded green rectangles. The red dots in the fluoroscopic images are the most extreme diaphragm and anterior-posterior position. The maximum motion amplitudes are determined by taking the difference between these most extreme points. ....3
- Figure 2. Lateral view of the digital mouse whole body phantom MOBY<sup>4</sup> and its Cartesian coordinate system, with several organs segmented.....4
- Figure 3. The diaphragm and AP motion amplitudes as a function of time obtained by fluoroscopic X-ray imaging of an anesthetized breathing mouse. Notice the long resting phase due to the use of anesthetic gas (isoflurane). .....5
- Figure 4. The average motion images over the whole 2.8 s breathing cycle of the eight MOBY simulation cases in left (L) and right (R) lung taking into account the derived breathing curve of an anesthetized mouse. The tumor is shown as a white sphere in all cases, the heart can only be seen in the left lung series as the white structure situated under the tumor. The white color of both tumor and heart is only used for visualization purposes, correct tissue values are assigned in the simulations. ....6
- Figure 5. The axial view of the MOBY phantom integrated in SmART-Plan showing the two different dose calculation methods. (a) a full 360° arc irradiation used to obtain the mean organ doses for each discrete time frame in the whole breathing cycle (b) 20 beams at different time points in the breathing phase are used to represent a full arc irradiation and to obtain time-dependent organ doses. ....7
- Figure 6. The real mouse tumor volume indicated in red (B) is used to create the MOBY tumor volume (A). The created MOBY lung tumor based on (B) is indicated by the green arrow, the white structures (heart and aorta) are only shown for visualization purposes. ....9
- Figure 7. The 'vascular system and heart' phantom in the axial (A), sagittal (B) and coronal (C) view..... 11
- Figure 8. The MOBY phantom consisting of one time frame is used in the contrast medium calculations. The MC tissues are assigned in the modified SmART-Plan code whereby no additional MOBY geometries should be created. ... 11
- Figure 9. The mean tumor dose delivered to each time frame of 50 ms during the breathing peak of 600 ms (Figure 3) for both right and left lung simulation cases..... 13

Figure 10. (A) the A-B dose profile line displayed on top of a MOBY simulation case. The tumor motion is indicated with a bold white arrow, and the incoming beam direction is indicated using the thin white arrow. (B) the final time-dependent dose distribution of the tumor in a Y,Z plane including the dose profile line A-B. (C)(D) the final A-B time-dependent tumor dose profiles of all simulation cases in right (C) and left (D) lung. .... 15

## Abbreviations

<b>3D</b>	Three-Dimensional
<b>4D</b>	Four-Dimensional
<b>AP</b>	Anterior Posterior
<b>BOT</b>	Beam On Time
<b>CBCT</b>	Cone Beam Computed Tomography
<b>CERT</b>	Contrast-Enhanced RadioTherapy
<b>EGS</b>	Electron Gamma Shower
<b>kV</b>	kiloVoltage
<b>MOBY</b>	digital mouse whole body phantom
<b>MC</b>	Monte Carlo
<b>NURBS</b>	Non-Uniform Rational B-Splines
<b>SARRP</b>	Small Animal Radiation Research Platform
<b>SmART-Plan</b>	Small Animal RadioTherapy plan
<b>STL</b>	STereoLithography
<b>TPS</b>	Treatment Planning System



## Abstract

During precision irradiation of a preclinical lung tumor model, the tumor is subject to breathing motion and it can partially move out of the irradiation field. This work aims to perform a quantitative analysis of the impact of respiratory motion on the irradiation with small fields of a mouse lung tumor and its surrounding normal tissues.

A 4D digital mouse whole body (MOBY) phantom with a virtual 4 mm spherical lung tumor at different locations in both lungs is used to simulate a breathing anesthetized mouse in different breathing phases representing a full breathing cycle. The breathing curve is determined by fluoroscopic imaging of an anesthetized mouse. Each MOBY time frame is loaded in a dedicated treatment planning system (SmART-Plan) and is irradiated by a full arc with a 5 mm circular collimator. Mean and time-dependent organ doses are calculated for the tumor, heart and spinal cord.

Depending on the location of the lung tumor, an overestimation of the mean tumor dose up to 11% is found. The mean heart dose could be both over (30%) or underestimated (14%) because the heart moves in or out of the irradiation field depending on the beam target location. The respiratory motion does not affect the mean spinal cord dose. A dose gradient is visible in the time-dependent tumor dose distribution.

In the future new methods need to be developed to track the lung tumor motion before pre-clinical irradiation to adjust the irradiation plan. Margins, collimator diameter and target dose could be changed easily, but they all have their drawbacks. State-of-the-art clinical techniques as respiratory gating or motion tracking may offer a solution for the cold spots in the time-dependent tumor dose.



## Abstract - Dutch

Tijdens de bestraling van een preklinisch longtumormodel kan de tumor zich gedeeltelijk uit het stralingsveld begeven omwille van de ademhalingsbeweging. Deze studie heeft als doel om kwantitatief te analyseren wat het effect is van ademhaling op een precisie longtumorbestraling bij muizen.

Een 4D digitaal muisfantoom (MOBY) met een virtuele sferische 4 mm longtumor op verschillende locaties in beide longen wordt gebruikt om een ademhalende muis te simuleren in verschillende ademhalingsfases. De ademhalingscurve van een geanestheerde muis wordt bepaald met behulp van fluoroscopie. Ieder MOBY tijdframe wordt ingeladen in een behandeling planningssysteem (SmART-Plan) en wordt via een boog bestraald met een 5 mm collimator. Gemiddelde en tijdsafhankelijke dosissen worden berekend voor de tumor, hart en ruggengraat.

Een overschatting van de gemiddelde tumordosis werd gevonden tot 11%, verschillend van de tumorpositie in de long. De gemiddelde hartdosis kan zowel over- als onderschat worden omdat het hart zich in of uit het stralingsveld kan begeven, afhankelijk van de targetpositie. De ademhalingsbeweging heeft geen invloed op de gemiddelde ruggengraatdosis. Een gradiënt is zichtbaar in de tijdsafhankelijke tumor dosisdistributie.

In te toekomst dienen methodes ontwikkeld te worden om de bestraling af te stemmen op de beweging van de longtumor. Marges, collimator diameter en targetdosis kunnen reeds gemakkelijk worden aangepast, maar hebben elk hun nadeel. Nieuwe klinische technieken zoals ademhaling gestuurde radiotherapie of tumor opvolging kunnen een oplossing bieden voor onderdosering in de tijdsafhankelijke distributie van de tumordosis.





# 1 Introduction

## 1.1 Dose perturbation in a moving mouse lung tumor

Small animal models are increasingly used in pre-clinical cancer radiobiology research to investigate the characteristics of cancer, e.g. tumor progression, metastases or hypoxia.<sup>1</sup> The combinational use of precision kilovolt X-ray irradiators and high resolution cone beam CT (CBCT) imaging systems provides an improvement of the accuracy in small animal image-guided radiotherapy.<sup>2</sup> Respiratory motion in small animals during image-guided precision irradiation is mentioned as a concern which has not yet been investigated in the literature.<sup>2</sup> Some organs could change position in the mouse as a function of time due to breathing which is not taken into account in currently available small animal precision irradiators.

While irradiating a mouse with a lung tumor in small animal precision radiotherapy, the tumor can partially move out of the small irradiation field so that certain regions of the tumor will not be irradiated for a small period of time. This issue is caused by the breathing motion and is more severe in small animals compared to human patients. First because mice are irradiated with precision beams using small margins between beam and target. Secondly because the relative displacement of the lung tumor will be larger in a mouse compared to a human. During the whole irradiation treatment there are multiple breathing cycles where the tumor can partially or completely move out of the irradiation field. Currently commercially available image-guided small animal radiation research systems such as the Xstrahl Ltd. (Camberley, Surrey, UK) small animal radiation research platform (SARRP) or the Precision X-ray Inc. (North Branford, CT, USA) X-Rad small animal radiotherapy (XRAD-SmART) do not provide an option to perform 4D CT imaging.<sup>3</sup> Therefore we cannot perform dose calculations on each 4D CT time frame as would be done for a human patient. In this work, we estimate the influence of breathing motion on the mean dose and the time-dependent dose in a mouse lung tumor irradiation in a mathematical phantom.

## 1.2 Contrast-enhanced small animal irradiations

Contrast agents contain high atomic number elements (e.g. iodine or gadolinium) which brings advantages in radiology. In contrast-enhanced radiotherapy (CERT) a dose fall-off is noticeable when contrast-enhanced tissues are irradiated with kilovolt X-rays (kV-CERT) which are used in the small animal radiation research systems. A dose enhancement is caused by the high cross sections for photo-electric effect for kilovolt X-rays in high atomic number elements.<sup>4</sup>

## 2 Methods

Figure 1 describes the workflow which will be explained in the following sections.

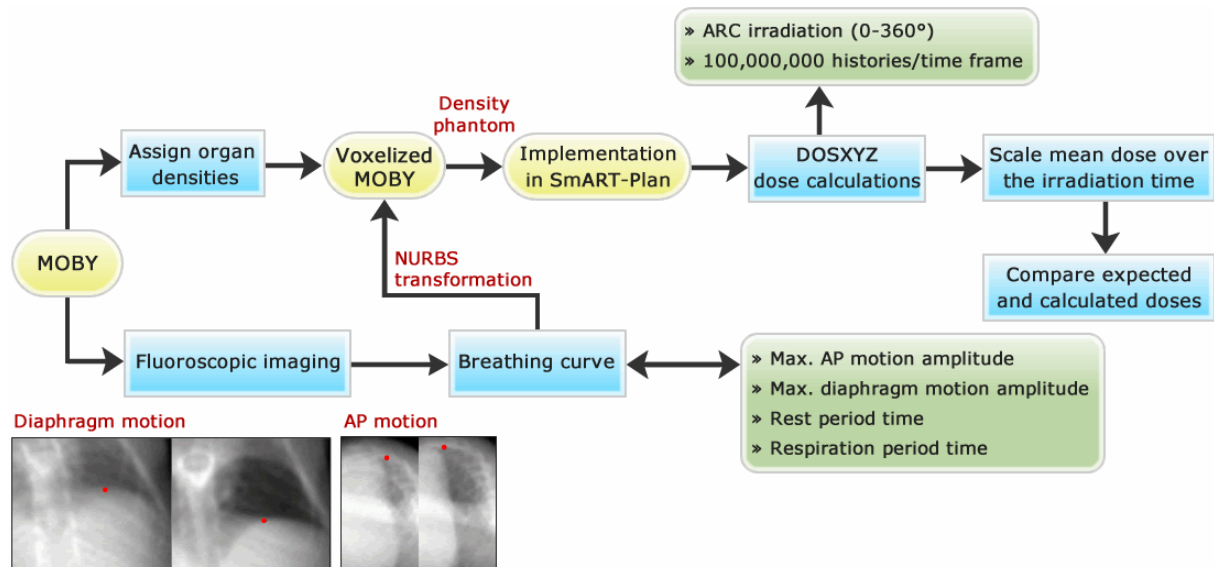


Figure 1. Flow diagram of the procedure to estimate lung tumor dose over time. The computer programs are shown in the rounded yellow rectangles, the methods in the blue rectangles and the parameters or settings in the partially rounded green rectangles. The red dots in the fluoroscopic images are the most extreme diaphragm and anterior-posterior position. The maximum motion amplitudes are determined by taking the difference between these most extreme points.

### 2.1 4D digital mouse whole body (MOBY) phantom

Figure 2 displays the MOBY phantom which is used to create a realistic and versatile respiratory model of the mouse anatomy.<sup>4</sup> Raw 32-bit binary output files are generated using the 'activity mode', where radionuclide activities for the various organs can be assigned in the input file. Instead of assigning activities, we assigned tissue densities to the organs listed in the activity mode. Due to the lack of small animal tissue data, human tissue densities and compositions<sup>5,6</sup> are assigned to the organ activity values. The assignment of tissue densities in the activity mode results in a MOBY phantom consisting of tissue densities.

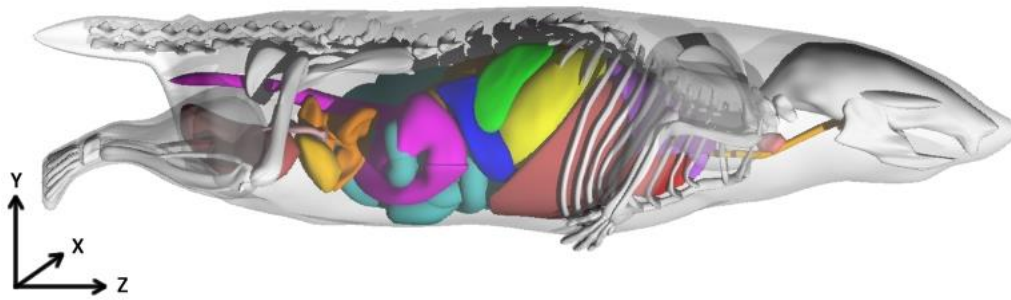


Figure 2. Lateral view of the digital mouse whole body phantom MOBY<sup>4</sup> and its Cartesian coordinate system, with several organs segmented.

Originally the breathing curve of a tidal breathing mouse without a resting phase was implemented in MOBY by the developers. This curve was obtained by monitoring time-dependent volume changes of a tidal breathing human, scaled to the dimensions of a mouse.<sup>7</sup> In pre-clinical research the mouse will be irradiated under the influence of anesthesia whereby the resulting breathing pattern will be slower and deeper, hence a new breathing curve must be obtained.

The respiratory motion of the phantom is modeled by a breathing curve which can be characterized by determining four parameters defined in the originally implemented curve: (i) maximum diaphragm motion amplitude, (ii) maximum anterior-posterior (AP) motion amplitude, (iii) rest period time and (iv) respiration period time. No left-right motion is modeled.

Fluoroscopic X-ray imaging of an anesthetized mouse is performed using the onboard imaging panel of the X-RAD 225Cx irradiator to determine the four parameters described above. Figure 3 illustrates a breathing curve derived from these measurements. The maximum AP amplitude, maximum diaphragm amplitude, rest period time and respiration period time are respectively found to be 2.0 mm, 4.0 mm, 2.2 s and 0.6 s. The diaphragm motion amplitude starts at 4.0 mm due to the negative Z diaphragm movement during inspiration according to the coordinate system in figure 2. Following the same reasoning the AP motion amplitude curve starts at the origin due to the positive Y movement during the inspiration phase.

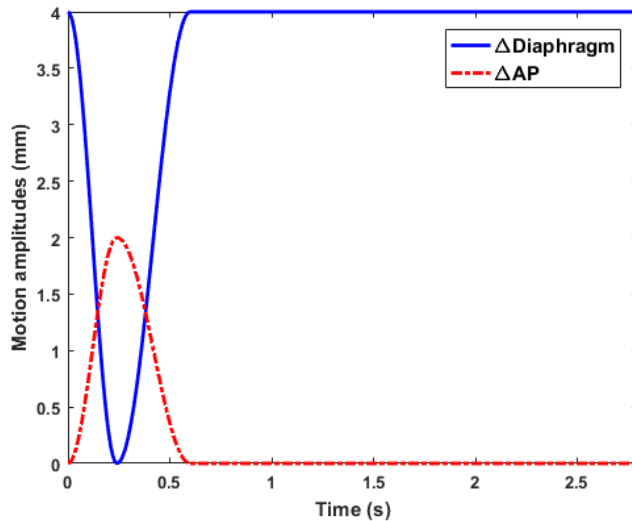


Figure 3. The diaphragm and AP motion amplitudes as a function of time obtained by fluoroscopic X-ray imaging of an anesthetized breathing mouse. Notice the long resting phase due to the use of anesthetic gas (isoflurane).

The full breathing curve is converted in non-uniform rational B-splines (NURBS) allowing the curve to be implemented in MOBY.<sup>8</sup> NURBS are preferred to model the respiratory motion because the curve parameters can be spline-interpolated in time to create a 4D phantom for any time interval.

As a final step the MOBY software samples the NURBS lung volume of the phantom in time frames consisting of 256x256x101 voxels with an isotropic size of 0.2 mm. The cubic voxel size determines the resolution of the resulting voxelized phantom. A total of 56 output frames represent a full breathing cycle of 2.80 s, in which each time frame represents a time interval of 50 ms.

## 2.2 MOBY simulation cases

A total of eight simulation cases are divided into: the right and left lung series. Each series of MOBY phantoms is created by placing the lung tumor at four different Z positions, while the X and Y initial coordinates of the lung tumor are the same throughout the creation of the series. The center of the 4 mm sphere lung tumor is displaced 2 mm in the positive Z direction for each following MOBY simulation case in the series.

Figure 4 shows eight average MOBY breathing phases obtained over the whole breathing cycle. Especially in the first and second case of both series the tumor movement in the negative Y and Z directions due to breathing can clearly be seen as a blurred tumor on the average motion images. This blurring, due to organ motion, is also visible in the average left lung images with respect to the heart.

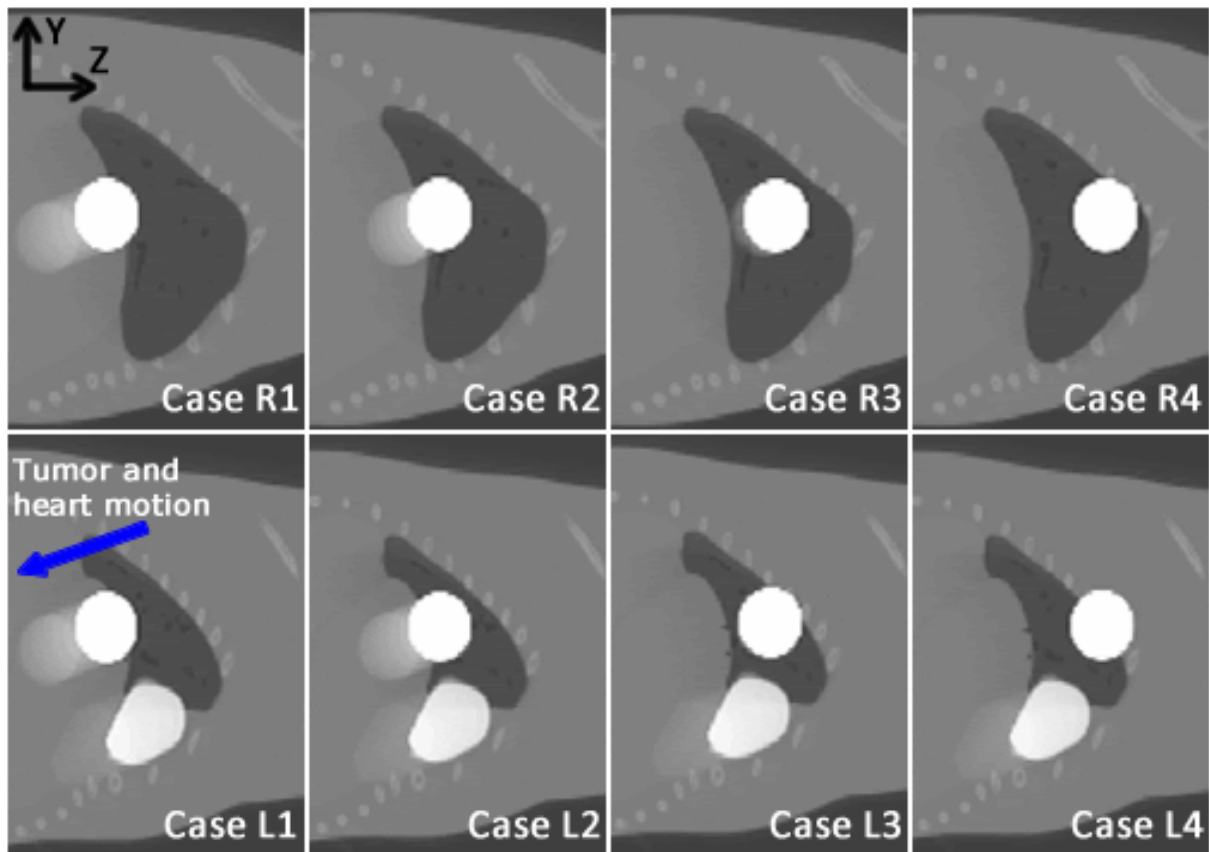


Figure 4. The average motion images over the whole 2.8 s breathing cycle of the eight MOBY simulation cases in left (L) and right (R) lung taking into account the derived breathing curve of an anesthetized mouse. The tumor is shown as a white sphere in all cases, the heart can only be seen in the left lung series as the white structure situated under the tumor. The white color of both tumor and heart is only used for visualization purposes, correct tissue values are assigned in the simulations.

### 2.3 SmART-Plan

SmART-Plan is a dedicated small animal radiotherapy treatment planning system (TPS) developed for use in pre-clinical research.<sup>9</sup> It is preferred over a clinical TPS considering the small voxel sizes, the small irradiation beams and the absence of kilovoltage X-ray beam models in a clinical TPS. Currently SmART-Plan does not allow dose calculations in moving mouse geometries.

SmART-Plan is modified using MATLAB (version R2012b, the MathWorks Inc., Natick, Massachusetts, USA) to perform dose calculations on all MOBY time frames constituting one breathing cycle. Full arc irradiations are performed to deliver an 8 Gy target dose to the lung tumor. In each case the beam is centered on the initial position of the tumor. By making use of SmART-Plan, Monte Carlo (MC) DOSXYZnrc dose calculations are executed on all MOBY time frames of each single case, taking into account the parameters listed in Table 1.<sup>10</sup> An isotropic margin of 0.5 mm is used to irradiate the tumor volume.

Table 1. Treatment and calculation settings of SmART-Plan combined with the MOBY phantom parameters to perform MC dose calculations.

SmART-Plan settings		MOBY parameters	
<b>Irradiation plan</b>	360° arc	<b>Time resolution</b>	50 ms
<b>Beam diameter</b>	5 mm	<b>Tumor diameter</b>	4 mm
<b>Planned target dose</b>	8 Gy	<b>Breathing curve</b>	Anesthetized mouse (Figure 3)
<b>Histories per frame</b>	100,000,000		

The final organ doses are determined in two different approaches (Figure 5): (i) the mean organ doses and (ii) the time-dependent organ doses. The organs for which dose is reported are the tumor, the heart and the spinal cord. Due to the changes in lung volume it is challenging to calculate mean and time-dependent lung doses.

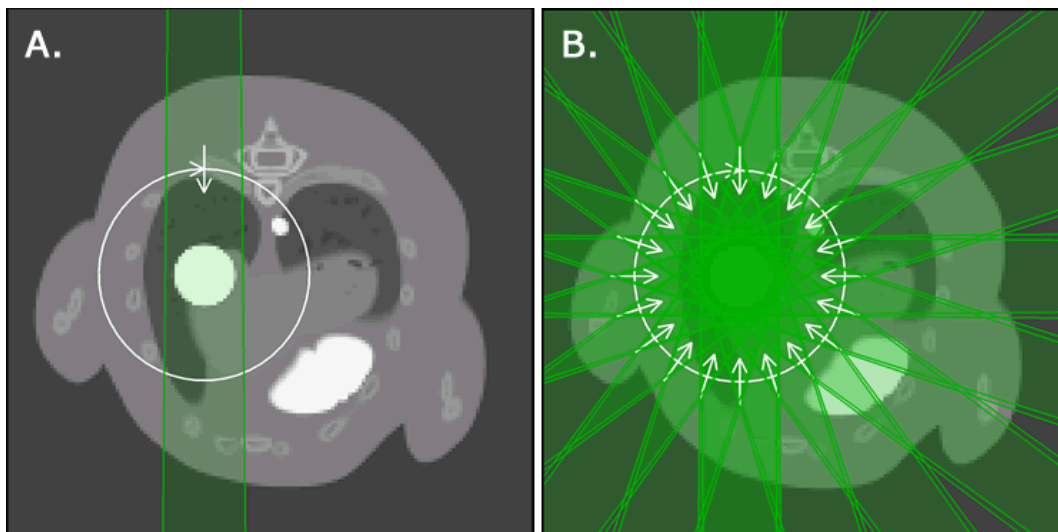


Figure 5. The axial view of the MOBY phantom integrated in SmART-Plan showing the two different dose calculation methods. (a) a full 360° arc irradiation used to obtain the mean organ doses for each discrete time frame in the whole breathing cycle (b) 20 beams at different time points in the breathing phase are used to represent a full arc irradiation and to obtain time-dependent organ doses.

### 2.3.1 Mean organ doses

Every static MOBY time frame is loaded separately in SMART-Plan. Each time frame is treated as a static geometry. Mean organ doses are determined in each time frame, hence a rescaling of the obtained mean organ doses is required to achieve dynamic mean organ doses taking into account the respiratory motion.

The rescaled value of the final mean organ dose  $D_{\text{organ}}$  is calculated according to following equation:

$$D_{\text{organ}} = \left( \sum_{i=1}^N \frac{D_{\text{organ},i}}{t_{\text{irr},i}} \cdot \Delta t \right) \cdot C_{\text{br}} \quad (1)$$

where  $N$  is the total number of MOBY time frames in one breathing cycle,  $D_{\text{organ},i}$  is the mean organ dose in time frame  $i$ ,  $t_{\text{irr},i}$  is the total irradiation time in time frame  $i$  estimated by SMART-Plan,  $\Delta t$  is the time interval of one MOBY frame and  $C_{\text{br}}$  is the total number of breathing cycles during the irradiation beam on time.

### 2.3.2 Time-dependent organ doses

This method to determine the dose distribution is more complicated because of the dynamic interplay between the motion of the gantry and the phantom. MC dose calculations are performed on the same eight MOBY simulation cases to obtain a more realistic dose distribution in the tumor, taking into account both breathing motion and gantry rotation. The SMART-Plan settings and the MOBY parameters remain the same, with the exception of the irradiation plan. The original 360° arc is now divided in 20 beams rotated 18 degrees relative to each other.

The respiratory period of the MOBY phantom only occurs during the breathing peak of 600 ms, which is represented by 13 MOBY time frames. Each of these MOBY time frames is loaded in SMART-Plan as a static geometry and is treated according to the modified irradiation plan. Dose calculations are performed for each beam of each MOBY time frame which results in a total number of 260 dose distributions. A time-dependent dose distribution of the tumor, heart and spinal cord can now be calculated by making use of these dose distributions in combination with the interrelationship between the organ displacement caused by breathing, the beam number and the MOBY time frame at specific time intervals.



## 2.4 Customized MOBY lung tumor volume

In the original MOBY software there is just one sphere tumor model available that could be modified in diameter and position. Sphere lung tumors are infrequent, most of the tumors have an irregular shape. A method is found using SmART-Plan, MATLAB and Rhinoceros 5 (NURBS modeling software) to convert a real delineated mouse lung tumor to a MOBY NURBS tumor volume.

First a micro CT scan of a real mouse is loaded in SmART-Plan. SmART-Plan is used to delineate the tumor volume in the lung. The three-dimensional (3D) binary mask of the delineated tumor volume is used to create a MATLAB isosurface. The isosurface combines the points with constant binary values to create a volume of space. This volume is converted in a stereolithography (STL) file format which can be loaded and modified in Rhinoceros 5. The lung tumor customization action plan in Rhinoceros is added in Appendix 1. The resulting NURBS volume can be loaded into the MOBY phantom (Figure 6), in which the position and size of the lung tumor can be changed easily because of the flexibility of the NURBS.

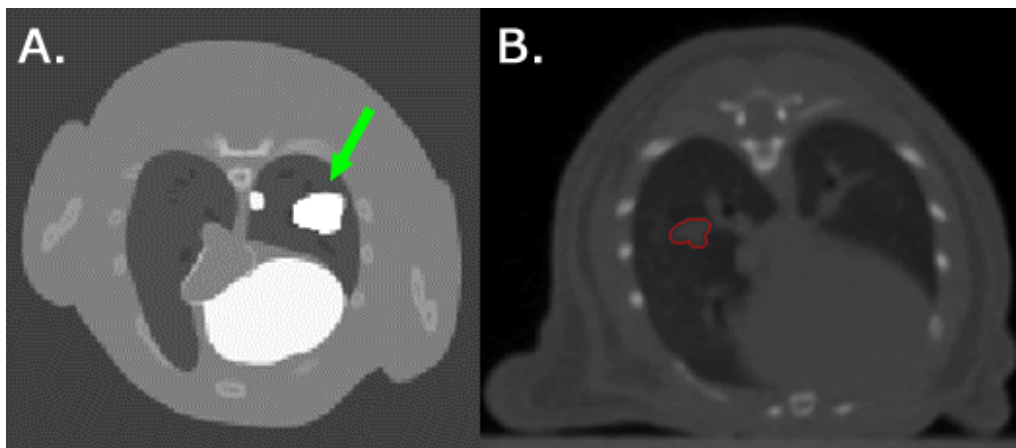


Figure 6. The real mouse tumor volume indicated in red (B) is used to create the MOBY tumor volume (A). The created MOBY lung tumor based on (B) is indicated by the green arrow, the white structures (heart and aorta) are only shown for visualization purposes.

## 2.5 Contrast-enhanced radiotherapy using MOBY

Omnipaque (300 mg I/ml) (Table 2) is injected in a lung tumor as X-ray imaging contrast medium.<sup>11</sup> In an ideal situation, the contrast medium remains in the injected tissue. Under real circumstances, a small amount of contrast medium will move from the lung tumor to the vascular system of the mouse. Due to the incomplete vascular system of the MOBY phantom that only consists of the thoracic and abdominal aorta, we assume a small amount of contrast medium displacement to the heart and the entire aorta.

Table 2: The mass density and atomic constituent weight fractions of the Omnipaque iodine based contrast medium.<sup>4</sup>

Omnipaque concentration	Mass density (g/cm <sup>3</sup> )	Atomic constituent				
		H	C	N	O	I
300 mg I/ml	1.338	0.073	0.134	0.025	0.544	0.224

Dose calculations are performed for six different contrast medium concentrations (100%, 90%, ..., 50%) and one reference condition without injected contrast medium, the six concentrations are diluted based on the original 300 mg I/ml Omnipaque concentration. The contrast enhanced tissue densities should be assigned to the MOBY density phantom, but the atomic weight fractions of these tissues are not mentioned in literature whereby new MC materials should be created. In this simulation: the contrast medium is diluted into a water tumor volume; a homogenous mixture is assumed and organ volume differences are ignored. The new contrast medium concentration in the tumor  $x'_{CM}$  is calculated according to following equation:

$$x'_{CM} = \frac{x_{CM} \cdot V_{CM}}{V_{CM} + V_w} \quad (2)$$

where  $x_{CM}$  is the injected contrast medium concentration into a tumor,  $V_{CM}$  and  $V_w$  are respectively the volumes of contrast medium and tumor (water).<sup>4</sup>

Based on this model new Electron Gamma Shower (EGS) materials are made in the graphical user interface of EGSnrcMP (Version 0.9, National Research Council of Canada). This newly created materials will then be assigned to a density value in the MOBY density phantom.

SmART-Plan is modified to perform dose calculations on the same MOBY geometry whereby the tumor, heart and aorta tissue compositions could be changed depending on the dilution percentage of the contrast medium.

Due to restrictions in automatic contouring, two different MOBY phantoms are used as input for the modified SmART-Plan software. Both MOBY phantoms are described below.

The first MOBY phantom only shows the vascular system and the heart (Figure 7), the second MOBY phantom shows a complete geometry comparable with the geometry used in the eight respiratory simulation cases. The vascular system and the heart of both geometries are the same, except for the visibility for automatic contouring.

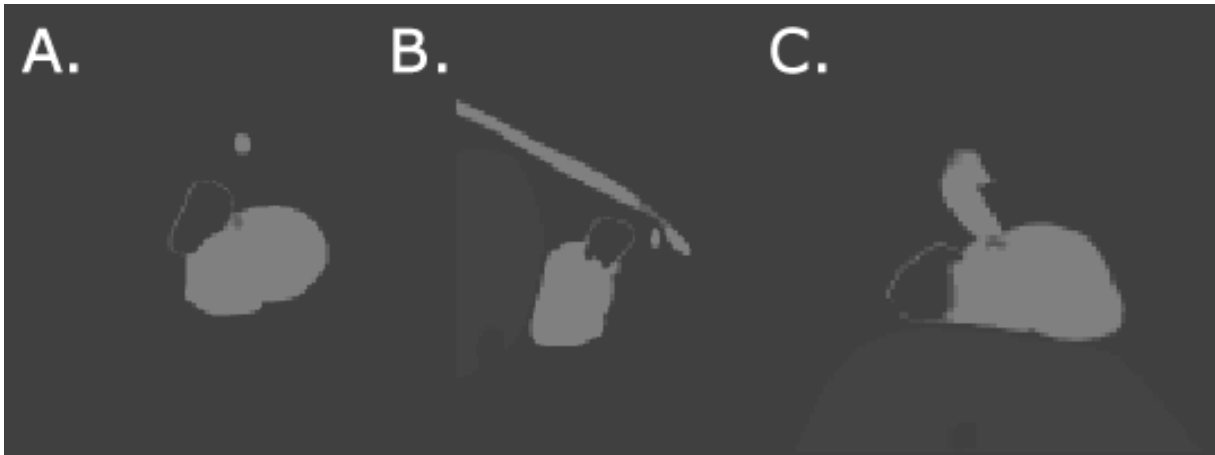


Figure 7. The 'vascular system and heart' phantom in the axial (A), sagittal (B) and coronal (C) view.

The resulting MOBY phantom (Figure 8) with a 3 mm spherical lung tumor is created without breathing motion (it consists of one time frame) and without cardiac pulses. The lung tumor is irradiated by a full 360° arc with a 5 mm circular collimator and an 8 Gy target (tumor) dose.

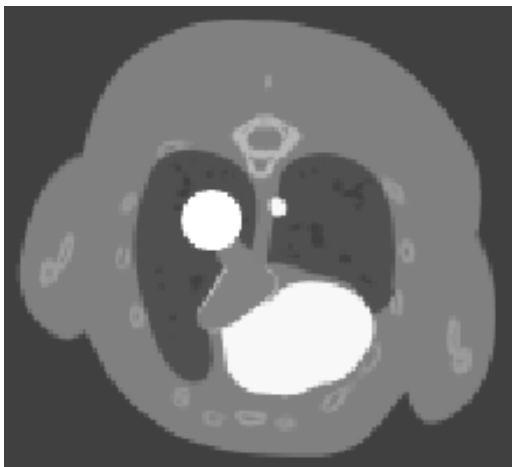


Figure 8. The MOBY phantom consisting of one time frame is used in the contrast medium calculations. The MC tissues are assigned in the modified SmART-Plan code whereby no additional MOBY geometries should be created.



### 3 Results

#### 3.1 Respiratory simulations: lung tumor displacement

The displacement of the center of mass of the lung tumor due to breathing is quantified for all MOBY simulation cases. The maximum three dimensional lung tumor displacement  $TD_{max}$  (Table 3) is calculated with the maximum Y and Z tumor displacement compared to the tumor position in the first MOBY time frame, respectively  $\Delta Y_{max}$  and  $\Delta Z_{max}$ . There is no measurable tumor displacement in the X direction all cases in both lungs.

Table 3. Maximum lung tumor displacements of all MOBY simulation cases in the Cartesian coordinate system. ( $TD_{max}^2=Y^2+Z^2$ )

	R series (mm)			L series (mm)		
	$\Delta Y_{max}$	$\Delta Z_{max}$	$TD_{max}$	$\Delta Y_{max}$	$\Delta Z_{max}$	$TD_{max}$
<b>Case 1</b>	-1.4	-3.9	4.1	-1.4	-3.9	4.1
<b>Case 2</b>	-1.0	-2.7	2.8	-1.2	-3.4	3.6
<b>Case 3</b>	-0.3	-0.9	1.0	-0.2	-0.2	0.3
<b>Case 4</b>	0.1	-0.1	0.1	0.1	-0.1	0.1

#### 3.2 Respiratory simulations: mean organ doses

During the arc irradiation in the 600 ms breathing peak, the mean tumor dose delivered in each MOBY time frame (50 ms) is shown in Figure 9. Only the breathing peak time interval is shown in the graph because the mean doses delivered in the rest phase do not change in time.

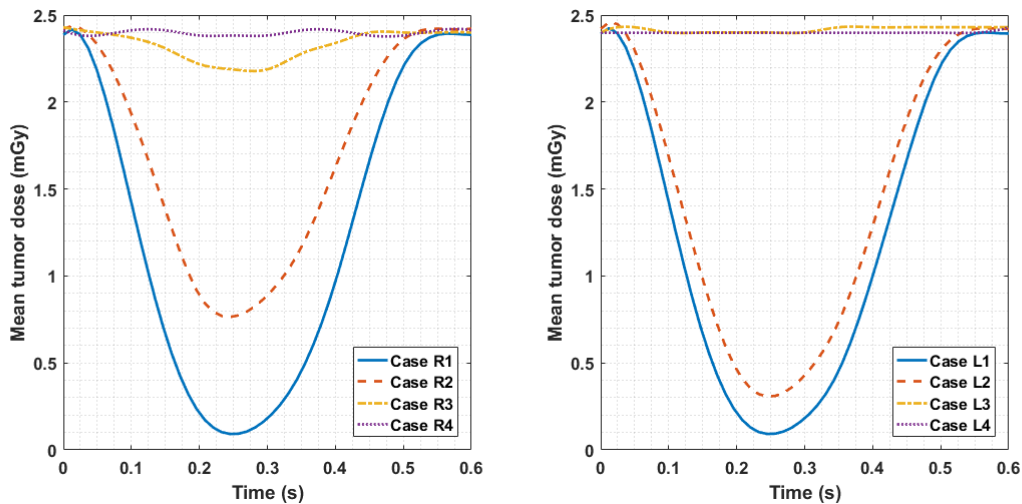


Figure 9. The mean tumor dose delivered to each time frame of 50 ms during the breathing peak of 600 ms (Figure 3) for both right and left lung simulation cases.

In the MOBY time frame with the most extreme motion amplitude, the tumor receives less than 5% of the prescribed target dose. This percentage will become larger with smaller motion amplitudes in the respiratory cycle. But in following representation, the obtained mean organ doses delivered to each MOBY time frame are averaged to a final mean organ dose over the full irradiation according to equation 1. Table 4 lists the rescaled mean organ doses delivered over the whole irradiation treatment to the tumor, heart and spinal cord. The obtained mean and expected mean doses are considered in a breathing and a non-breathing MOBY phantom, respectively. Relative differences are determined between the obtained and expected mean organ doses. This provides insight in the percentage over (-) or underestimation (+) of the mean organ dose due to respiratory motion.

Table 4. The expected (static) and obtained (moving) mean dose for the tumor, heart and spinal cord of all simulation cases in both right (R) and left (L) lung.

	<b>Expected (Gy)</b>	<b>Obtained (Gy)</b>	<b>Difference %</b>	<b>Expected (Gy)</b>	<b>Obtained (Gy)</b>	<b>Difference %</b>
	<b>Case R1</b>			<b>Case L1</b>		
Tumor	7.93	7.09	-11	7.92	7.09	-11
Heart	0.40	0.52	30	0.51	0.64	25
Spinal cord	0.69	0.69	0	0.70	0.70	0
	<b>Case R2</b>			<b>Case L2</b>		
Tumor	7.91	7.40	-6	7.91	7.22	-9
Heart	1.18	1.15	-3	1.46	1.40	-4
Spinal cord	0.80	0.81	1	0.78	0.78	0
	<b>Case R3</b>			<b>Case L3</b>		
Tumor	7.95	7.89	-1	7.95	7.94	0
Heart	1.30	1.15	-12	1.55	1.36	-12
Spinal cord	0.99	0.99	0	0.90	0.90	0
	<b>Case R4</b>			<b>Case L4</b>		
Tumor	7.96	7.96	0	7.94	7.93	0
Heart	0.51	0.44	-14	0.58	0.50	-14
Spinal cord	1.22	1.21	-1	1.02	1.02	0

### 3.3 Respiratory simulations: time-dependent organ doses

A dose profile along the line A-B in Figure 10A is determined at the position where the spherical tumor has its maximum diameter in the final time-dependent dose distribution over the whole irradiation treatment. These dose profiles were extracted for each case in the right and left lung series, the results are shown in Figure 10. Only the dose gradient of Case R1 is shown (Figure 10B) to obtain a better understanding of the time-dependent dose profiles in Figure 10 C-D. Underdosage in the tumor of up to 23% can be seen in the volume that will move out of the irradiation field first. This difference is decreasing if the tumor moves out of the irradiation field for a shorter period of time. The dose gradients for both lung series in the Y,Z plane are shown Figure 10 C-D.

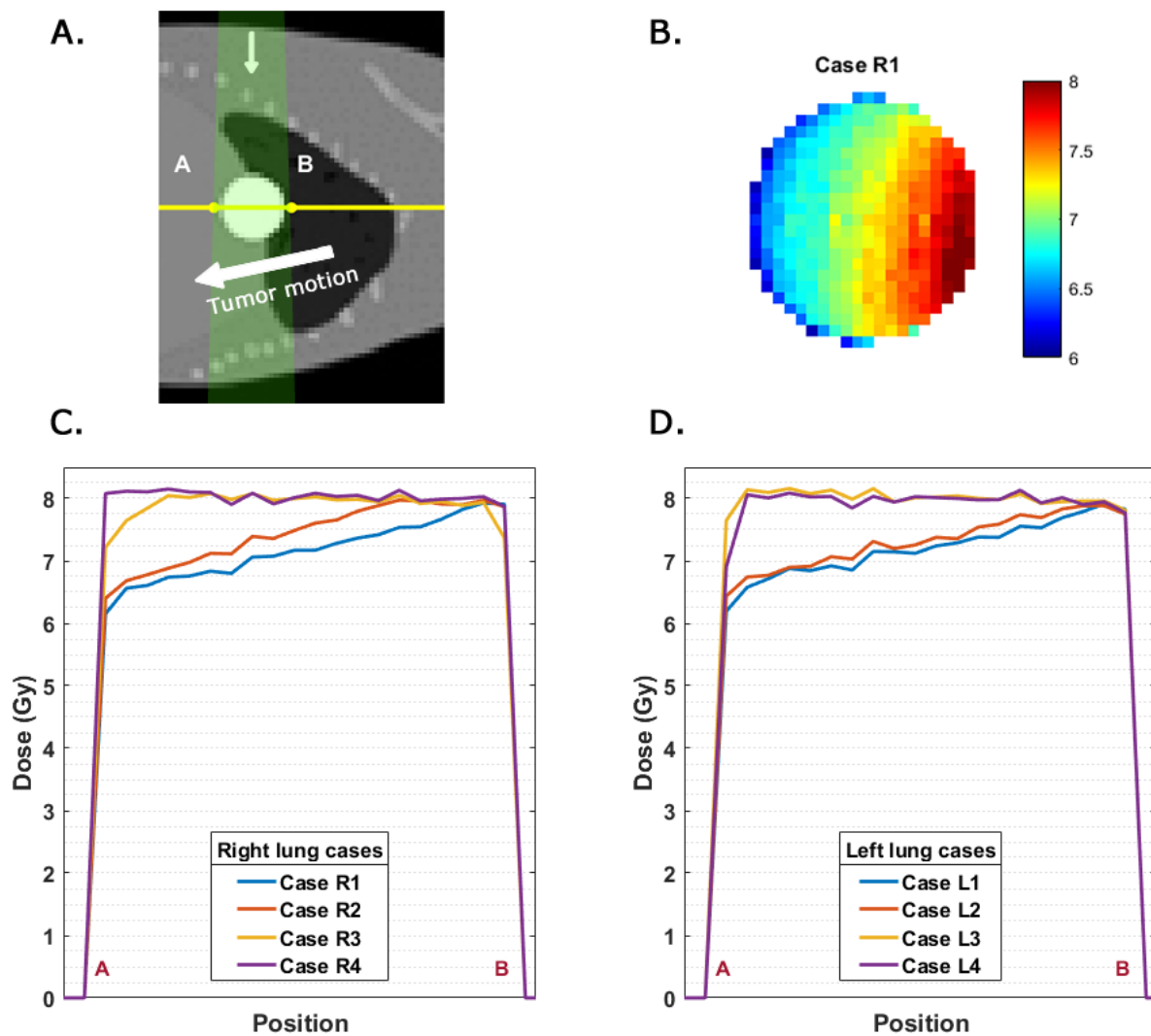


Figure 10. (A) the A-B dose profile line displayed on top of a MOBY simulation case. The tumor motion is indicated with a bold white arrow, and the incoming beam direction is indicated using the thin white arrow. (B) the final time-dependent dose distribution of the tumor in a Y,Z plane including the dose profile line A-B. (C)(D) the final A-B time-dependent tumor dose profiles of all simulation cases in right (C) and left (D) lung.

### 3.4 Contrast-enhanced radiotherapy simulations

The results of the seven CERT MOBY simulation cases are listed in Table 5. Mean heart and tumor doses are calculated for the reference case and for the six different Omnipaque contrast medium dilutions. The estimated Beam On Time (BOT) is calculated by SmART-Plan for each contrast medium simulation case and is used to calculate the dose rate (DR) for both the tumor and heart.

Table 5. The calculated mean tumor and heart dose for all seven simulation cases with a planned treatment target dose of 8 Gy.

<b>Experiment</b>	<b><math>D_{\text{tumor}}</math> (Gy)</b>	<b><math>D_{\text{heart}}</math> (Gy)</b>	<b><math>BOT</math> (s)</b>	<b><math>DR_{\text{tumor}}</math> (mGy/s)</b>	<b><math>DR_{\text{heart}}</math> (mGy/s)</b>
<b>Reference</b>	7.9	2.1	165.7	47.7	12.7
<b>100%</b>	9.0	0.0	10.5	857.1	0.0
<b>90%</b>	9.0	0.2	10.1	891.1	19.8
<b>80%</b>	8.8	0.4	10.8	814.8	37.0
<b>70%</b>	8.6	0.5	11.8	728.8	42.4
<b>60%</b>	8.5	0.8	13.1	648.9	61.1
<b>50%</b>	8.3	0.8	14.7	564.6	54.4



## 4 Discussion

### 4.1 Dose perturbation in a moving mouse lung tumor

The breathing motion amplitude of the mouse lung tumor strongly depends on its position in the lung. This amplitude is larger at tumor locations near the diaphragm and smaller at tumor locations near the top of the lung. For the two superiorly-placed cases of the left and right lung series, the tumor displacement and tumor dose difference are sufficiently small to be ignored. This is caused by a combination of the tumor diameter (4 mm), the circular field diameter (5 mm) and the small motion amplitudes ( $\sim 0.1$  mm), ensuring the radiation field encompasses the tumor at all times. In this study only motion in the Y and Z directions are modeled, in accordance with mouse breathing measurements. Therefore no motion in the X direction is modeled.

When the static dose calculation is compared to the one taking into account motion, the former overestimates the mean tumor dose by up to 11%. This adverse overestimation of the mean tumor dose due to breathing increases at lower tumor position in the lung. In case of the heart, the relative difference of the mean heart dose strongly depends on the lung tumor position (range -14% to +30%). The tumor movement is smaller at higher lung tumor positions although the heart displacement remains the same in all simulation cases. No cardiac pulses are modeled in the heart, the displacement of the heart is only caused by breathing in this model. Depending on the lung tumor and therefore the target position, the heart moves in or out of the small radiation beam. Mainly in the superior lung tumor positions, the heart moves out of the radiation beam which results in an overestimation in the mean heart dose. The relative differences of the mean organ doses are consistent for both lungs taking into account the absolute tumor displacement, although the mean heart doses are larger when the tumor is situated in the left lung. In all simulation cases the mean spinal cord dose remains constant during the irradiation treatment.

The time-dependent tumor dose distribution has the advantage that cold spots are visualized which was not feasible with the mean dose rescaling method. A gradient in the Z direction is noticeable in the dose section lines of the slice with a maximum tumor diameter. A steeper dose gradient is present when the tumor is located near the diaphragm, which decreases when the tumor is located higher in the lung. When the tumor is located at the top of the lung the dose distribution is almost homogeneous. Cold spots are first visible in the region where the tumor starts to move out the irradiation field. The dose reduction in a tumor voxel is proportional to the time it is out of the irradiation field.

The tumor underdosage can be corrected by increasing the planned target dose. However, the tumor dose heterogeneity would still be present. The dose gradient can be avoided by irradiating the tumor with a collimator size equal to the tumor radius plus the maximum tumor displacement. A drawback of this approach is that the dose delivered to the surrounding organs will be increased significantly (Appendix 2).

Using state of the art techniques such as respiratory gating<sup>12</sup> or motion tracking allows for the delivery of uniform dose distributions to the tumor without delivering higher doses to surrounding normal tissues. These techniques are not yet available in image-guided small animal radiation research platforms. Studies like ours can provide guidelines for treatment margins to avoid underdosing target structures.

All the results in this work are obtained using one derived breathing pattern of an anesthetized mouse and one irradiation plan with different tumor positions in the left and right lung. It should be noted that the results will depend on the species, type of anesthesia, tumor position and irradiation plan.

## 4.2 Contrast-enhanced small animal irradiations

The reference calculation without any contrast medium in the kV-CERT dose calculations listed in Table 5 is more realistic compared to the dose calculations of the six contrast medium dilutions. The estimated BOT's become smaller and the target dose becomes larger when the tumor is injected with a larger concentration of Omnipaque contrast medium. These experiments show the expected results based on the literature available about kV-CERT, but the BOT's of this simulations are not realistic.<sup>4</sup> For the small animal irradiator it will be hard to perform a full arc irradiation of mouse in 10 seconds with high tumor dose rates.

These dose calculations need careful thinking about how to report the dose in high atomic number mediums (e.g. iodine) in: dose to water or dose to medium. In vivo tumor experiments should be performed to see if the tumor growth depends on dose to medium or dose to water. Following studies in kV CERT are beyond the scope of this master's thesis and could be further investigated in the future.

## 5 Conclusion

Usage of the mathematical motion phantom MOBY in combination with a small animal treatment planning system SMART-Plan provides a suitable method to quantify the dose reduction due to respiratory motion in a mouse lung tumor irradiation, based on mean doses.

Some differences between the expected and obtained mean tumor doses are large enough to take into account in small animal treatment planning of lung tumors. Especially in cases where the lung tumor is located near the diaphragm of the mouse because the tumor displacement will be larger.

We recommend assessing the tumor motion of animal specimens using e.g. fluoroscopic imaging under treatment anesthesia, before performing small animal precision irradiation. In absence of gating or tracking techniques, fluoroscopic imaging can be used to determine appropriate treatment margins covering the lung tumor motion.



## References

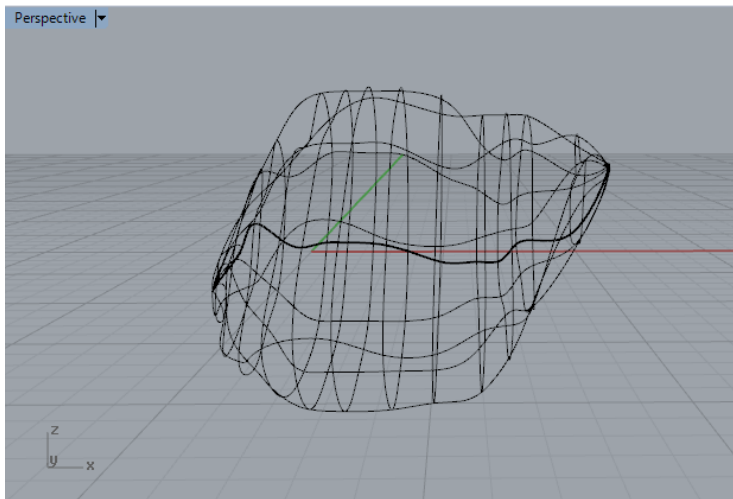
1. Tillner, F., Thute, P., Büttof, R., Krause, M. & Enghardt, W. Pre-clinical research in small animals using radiotherapy technology - a bidirectional translational approach. *Z. Med. Phys.* **24**, 335–351 (2014).
2. Verhaegen, F., van Hoof, S., Granton, P. V. & Trani, D. A review of treatment planning for precision image-guided photon beam pre-clinical animal radiation studies. *Z. Med. Phys.* **24**, 323–334 (2014).
3. Verhaegen, F., Granton, P. & Tryggestad, E. Small animal radiotherapy research platforms. *Phys. Med. Biol.* **56**, R55–R83 (2011).
4. Verhaegen, F. *et al.* Dosimetric and microdosimetric study of contrast-enhanced radiotherapy with kilovolt x-rays. *Phys. Med. Biol.* **50**, 3555–69 (2005).
5. International Commission on Radiation Units and Measurements. Tissue substitutes in radiation dosimetry and measurement. *ICRU Rep. 44* (1988).
6. Schneider, U., Pedroni, E. & Lomax, A. The calibration of CT Hounsfield units for radiotherapy treatment planning. *Phys. Med. Biol.* **41**, 111–24 (1996).
7. Segars, W. P., Tsui, B. M. W., Frey, E. C., Johnson, G. A. & Berr, S. S. Development of a 4D digital mouse phantom for molecular imaging research. *Mol. Imaging Biol.* **6**, 149–159 (2004).
8. Beer, G. & Bordas, S. *Isogeometric Methods for Numerical Simulation*. (Springer-Verlag GmbH, 2015). doi:10.1007/978-3-7091-1843-6\_2
9. Van Hoof, S. J., Granton, P. V. & Verhaegen, F. Development and validation of a treatment planning system for small animal radiotherapy: SmART-Plan. *Radiother. Oncol.* **109**, 361–366 (2013).
10. Walters, B., Kawrakow, I. & Rogers, D. W. O. DOSXYZnrc Users Manual. *NRCC Rep. PIRS-0794* 1–125 (2013).
11. GE Healthcare. *Omnipaque (iohexol) Information sheet*. (2010).
12. Tami Freeman. Introducing gating to small-animal irradiation. (2016). Available at: <http://medicalphysicsweb.org/cws/article/opinion/64601>. (Accessed: 15th April 2016)



## Appendix 1 – Customized MOBY tumor action plan

1. Select the imported mesh volume, type 'meshtonurb' in the command line and press enter.
2. Now you have a mesh volume and a polysurface. Select and delete the mesh surface so that only the latter remains.
3. Place 1 point at the beginning and 1 point at the end of the polysurface. Check if the points are in a proper 3D location by looking in all views. Later, these points will be used as start and ending points of the NURBS volume.
4. Type 'sections' in the command line and press enter. Select the volume and press enter again. Now you can define "slices/sections" of the volume. It is important to follow the instructions of the command line! The start and the endpoints of the section can be defined outside the volume. Rhinoceros will search for the volume and takes the crossing points as start and ending points. Define enough slices through the volume. When all sections are drawn press enter or escape.
5. Further steps will be more clear when the polysurface is deleted. Only the sections are remaining in the Rhino workspace. Check if the sections are a closed area. If the sections are built by multiple smaller sections they have to be joined. Select one section region (consists of multiple sections in the same plane), type 'Join' in the command line and press enter. Do this for all section lines.
6. Type 'Loft' in the command line and press enter. First select the starting point and go on with the remaining sections in correct sequential order, then select the ending point and press enter. If you have to choose between curves during the 'loft' selection, the procedure has gone wrong. After the selection of the ending point a 'Loft Options' menu appears. Use the normal style and rebuild the volume with the desired number of control points. There is a possibility to have a preview of the created surface. Press OK when you have the desired volume.
7. Select the surface and type 'makenonperiodic' in the command line. Press enter.

8. Further steps will be more clear when the sections and both points are deleted. Only the created volume is retained in the workspace. Be sure that the volume is located in the center. You can check this by typing 'VolumeCentroid' in the command line.
9. To create a NURBS volume which is compatible with MOBY, you have to use a Rhinoceros script called 'OutputNurbs2'. If you never used this Rhinoceros script before, you have to drag and drop it in the command line. Now select the NURBS surface and type 'OutputNurbs2' in the command line. Choose a filename and click on save.



Appendix 1. An example of a resulting NURBS volume shown in Rhinoceros 5 after completing previous steps. This volume is used in the MOBY phantom tumor customization process.

10. A .NRB file is created. Be sure there are no commas in the output file. If there are commas: find and replace them by points. Otherwise the MOBY phantom creation will fail (error: core dumped).
11. Drag and drop the created lesion .NRB file in the standard MOBY folder.



## Appendix 2 – Mean obtained organ doses calculated using a larger 10 mm collimator

The mean organ doses are calculated using the same MOBY settings and SmART-Plan parameters with the exception of a larger circular collimator of 10 mm instead of 5 mm.

Appendix 2. The obtained mean organ doses over the whole irradiation treatment, in case of a breathing MOBY phantom, are calculated using a 10 mm circular collimator instead of 5 mm which was used in previous mean organ dose calculations. The absolute differences (in Gy) are calculated between the obtained doses using a 5 mm and a 10 mm collimator diameter.

	Obtained (Gy) D <sub>coll</sub> =5 mm	Obtained (Gy) D <sub>coll</sub> =10 mm	Absolute difference (Gy)	Obtained (Gy) D <sub>coll</sub> =5 mm	Obtained (Gy) D <sub>coll</sub> =10 mm	Absolute difference (Gy)
	<b>Case R1</b>			<b>Case L1</b>		
Tumor	7.09	7.84	0.75	7.09	7.83	0.74
Heart	0.52	2.58	2.06	0.64	3.16	2.52
Spinal cord	0.69	2.81	2.12	0.70	2.76	2.06
	<b>Case R2</b>			<b>Case L2</b>		
Tumor	7.40	7.95	0.55	7.22	7.90	0.68
Heart	1.15	3.38	2.23	1.40	4.09	2.69
Spinal cord	0.81	3.50	2.69	0.78	3.34	2.56
	<b>Case R3</b>			<b>Case L3</b>		
Tumor	7.89	7.98	0.09	7.94	7.97	0.03
Heart	1.15	3.30	2.15	1.36	3.95	2.59
Spinal cord	0.99	4.30	3.31	0.90	3.78	2.88
	<b>Case R4</b>			<b>Case L4</b>		
Tumor	7.96	7.99	0.03	7.93	7.97	0.04
Heart	0.44	2.39	1.95	0.50	2.81	2.31
Spinal cord	1.21	4.94	3.73	1.02	4.18	3.16

The overestimation of the tumor dose can be avoided by using a larger collimator diameter which covers the maximum tumor displacement plus the tumor radius. As a drawback, the mean doses delivered to the surrounding tissues are much larger.

## **Auteursrechtelijke overeenkomst**

Ik/wij verlenen het wereldwijde auteursrecht voor de ingediende eindverhandeling:

**The influence of respiratory motion on dose delivery in a mouse lung tumor irradiation using the 4D MOBY phantom**

Richting: **master in de industriële wetenschappen: nucleaire technologie-nucleaire technieken / medisch nucleaire technieken**

Jaar: **2016**

in alle mogelijke mediaformaten, - bestaande en in de toekomst te ontwikkelen - , aan de Universiteit Hasselt.

Niet tegenstaand deze toekenning van het auteursrecht aan de Universiteit Hasselt behoud ik als auteur het recht om de eindverhandeling, - in zijn geheel of gedeeltelijk -, vrij te reproduceren, (her)publiceren of distribueren zonder de toelating te moeten verkrijgen van de Universiteit Hasselt.

Ik bevestig dat de eindverhandeling mijn origineel werk is, en dat ik het recht heb om de rechten te verlenen die in deze overeenkomst worden beschreven. Ik verklaar tevens dat de eindverhandeling, naar mijn weten, het auteursrecht van anderen niet overtreedt.

Ik verklaar tevens dat ik voor het materiaal in de eindverhandeling dat beschermd wordt door het auteursrecht, de nodige toelatingen heb verkregen zodat ik deze ook aan de Universiteit Hasselt kan overdragen en dat dit duidelijk in de tekst en inhoud van de eindverhandeling werd genotificeerd.

Universiteit Hasselt zal mij als auteur(s) van de eindverhandeling identificeren en zal geen wijzigingen aanbrengen aan de eindverhandeling, uitgezonderd deze toegelaten door deze overeenkomst.

Voor akkoord,

**van der Heyden, Brent**

Datum: **4/06/2016**